Inorganic Chemistry

Article

pubs.acs.org/IC

Carbide Clusterfullerene $Gd_2C_2@C_{92}$ vs Dimetallofullerene $Gd_2@C_{94}$: A Quantum Chemical Survey

Yi-Jun Guo,[†] Tao Yang,[†] Shigeru Nagase,[‡] and Xiang Zhao*[,†]

[†]Institute for Chemical Physics & Department of Chemistry, State Key Laboratory of Electrical Insulation and Power Equipment, Xi'an Jiaotong University, Xi'an 710049, China

[‡]Fukui Institute for Fundamental Chemistry, Kyoto University, Kyoto 606-8103, Japan

Supporting Information

ABSTRACT: The geometric, electronic structure, and thermodynamic stability of Gd_2C_{94} species, including dimetallofullerenes $Gd_2@C_{94}$ and carbide clusterfullerenes $Gd_2C_2@C_{92}$, have been systematically investigated by a density functional theory approach combined with statistical mechanics calculations. Although the $Gd_2@C_2(153480)$-C_{94} is determined to possess the lowest energy, its molar fraction at the temperature region of fullerene formation is extremely low if the temperature effect is taken into consideration. Meanwhile, three C_{92}-based carbide clusterfullerene species, $Gd_2C_2@D_3(126408)$-C_{92}, $Gd_2C_2@C_1(126390)$-C_{92}, and $Gd_2C_2@C_2(126387)$-C_{92}, with some higher energy are exposed to possess considerable thermodynamic stabilities within a related temperature interval, suggesting that carbide clusterfullerenes rather than dimetallofullerenes could be isolated experimentally. Although one isomer, $Gd_2C_2@D_3(126408)$-C_{92}, has been indeed obtained experimentally, a novel structure, $Gd_2C_2@C_1(126390)$-C_{92}, behaving as the most abundant isomer at more elevated temperatures with the largest SOMO−LUMO gap, is predicted for the first time to be another proper isomer isolated in the experiment. Moreover, in order to further analyze the interaction between gadolinium atoms and carbon atoms in either a carbide cluster or a fullerene cage, frontier molecular orbital, natural bond orbital, and Mayer bond order analyses have been employed, and the results show that the covalent interaction cannot be neglected. The IR spectra of $Gd_2C_2@C_{92}$ have been simulated to provide some valuable guidance for future experiments.

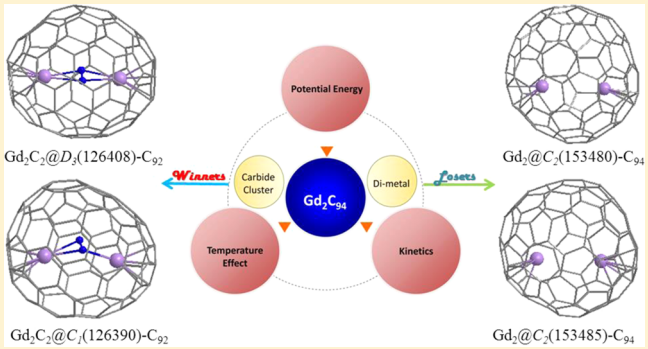

INTRODUCTION

In 1991, with the successful synthesis and separation of La@C_{82},[1] a novel kind of compound, endohedral metallofullerenes (EMFs), were generated. Since then, EMFs have attracted sights all over the world just for their novel structures and fascinating properties,[2−7] and a great deal of applications in many fields, including biomedicine, electronics, photovoltaics, and materials science,[8−12] have been predicted and realized. It is now acknowledged that EMFs can be classifiable into three types according to the form of the encapsulated species: mono-EMFs, di-EMFs, and metallocluster EMFs.

As one special type of EMFs, dimetallofullerenes with two metal atoms inside fullerene cages have been synthetized since the very early years of EMF researches; however, their yields are relatively low[13] compared with those of monometallofullerenes. Consequently, the characterization of dimetallofullerenes remains rather difficult, and dimetallofullerenes were considered to be the unique form of EMFs M_2C_{2n} at that time. In 2001, a breakthrough appeared that a ^{13}C NMR spectroscopic study of "$Sc_2@C_{86}$" indicated that the cage structure should be C_{84}. Hence, "$Sc_2@C_{86}$" was proposed to be $Sc_2C_2@C_{84}$.[14] From then on, another kind of EMF, carbide clusterfullerenes, was discovered. Later, some other carbide clusterfullerenes, such as $Sc_2C_2@C_{80}$,[15] $Sc_2C_2@C_{82}$,[16] and $Y_2C_2@C_{84}$,[17] have been isolated and studied. Noteworthy, the $Y_2C_2@C_{84}$ becomes the first dimetal carbide cluster endohedral fullerene violating the famous isolated pentagon rule (IPR).[19]

Obviously, endohedral fullerenes M_2C_{2n} could exist as two distinguished forms: dimetallofullerene $M_2@C_{2n}$ and carbide clusterfullerenes $M_2C_2@C_{(2n-2)}$. Consequently, structural determination of M_2C_{2n} must be very careful. $Sc_2C_2@C_{2v}(6073)$-C_{68}[18] was previously attractive because it had been the first carbide clusterfullerene violating the well-known IPR. Nevertheless, according to a very recent report,[20] a conventional dimetallofullerene $Sc_2@C_{70}$ is much more stable than $Sc_2C_2@C_{68}$ in terms of both thermodynamic and kinetic aspects, which revealed that $Sc_2@C_{70}$, rather than $Sc_2C_2@C_{68}$, is a better choice for Sc_2C_{70}. In addition, Ti_2C_{80} was originally considered as "$Ti_2@C_{80}$", and in 2001, its ^{13}C NMR spectrum was interpreted as a mixture of $D_{5h}(6)$-C_{80} and $I_h(7)$-C_{80} isomers with the ratio of 3:1.[21] In 2005, computational studies have

Received: September 10, 2013
Published: February 4, 2014

   dx.doi.org/10.1021/ic4022933 | Inorg. Chem. 2014, 53, 2012−2021

shown that $Ti_2C_2@D_{3h}$-(5)C_{78} is much more stable and also better fits for the ^{13}C NMR spectrum.[22,23] Other examples include $Sc_2C_2@C_{2v}$(5)-C_{80} rather than $Sc_2@C_{82}$,[24] $Sc_2C_2@C_s$(6)-C_{82} rather than $Sc_2@C_s$(10)-C_{84},[25] $Sc_2C_2@C_{3v}$(8)-C_{82} rather than $Sc_2@D_{2d}$(23)-C_{84},[26], etc. Consequently, when M_2C_{2n} is studied, two kinds of structures (i.e., $M_2@C_{2n}$ and $M_2C_2@C_{(2n-2)}$) should be considered simultaneously.

A family of gadolinium-containing EMFs were synthesized by Liu, Balch, and co-workers in 2008.[27] By using the high-pressure liquid chromatography (HPLC) and mass spectrometric analysis, two different isomers of Gd_2C_{94} were found, named as Gd_2C_{94} (I) and Gd_2C_{94} (II), respectively. Crystallographic characterization of Gd_2C_{94} (I) revealed that it possesses a carbide structure, $Gd_2C_2@D_3$(126408)-C_{92}, which is the largest carbide clusterfullerene characterized experimentally so far.[28] It should be noted that the $Gd_2C_2@D_3$(85)-C_{92} isomer mentioned in ref 27 is just the $Gd_2C_2@D_3$(126408)-C_{92} one here, as a more general description in the form of spiral numbers are used, instead of the IPR numbers in their report. On the other hand, another structure, Gd_2C_{94} (II), is still ambiguous.

Indeed, both $M_2C_2@C_{(2n-2)}$ and $M_2@C_{2n}$ were considered in the previous study. On the one hand, Popov and Dunsch[29] calculated the hexa-anions of the C_{94} isomers satisfying the IPR and predicted the isomer C_2(153480)-C_{94} to be the best candidate for the nitride clusterfullerenes. On the basis of their results, Yang et al. proposed $Gd_2@C_2$(153480)-C_{94} to be the most possible candidate for the conventional dimetallofullerene $Gd_2@C_{94}$. On the other hand, regarding the computational results shown by Yang et al.,[27] the C_1(126390)-C_{92} cage appears to be a likely candidate for the $M_2C_2@C_{(2n-2)}$ structure due to its relatively large (LUMO-3)−(LUMO-2) gap.[30] By comparing the potential energy between $Gd_2C_2@C_1$(126390)-C_{92} and $Gd_2@C_2$(153480)-C_{94}, Yang and co-workers finally suggested that $Gd_2@C_2$(153480)-C_{94} should be more superior.

Nevertheless, in their work, IPR isomers were taken into consideration only, and non-IPR isomers that may be of great contribution in some EMFs were ignored. In 2011, a theoretical report[31] pointed out that metal atoms encapsulated in the fullerene cage might stabilize the fused pentagons and even enhanced the relative stability of metallofullerenes. More importantly, a general rule that explains the reason why the charged cages violating IPR and the non-IPR EMFs may be more stable than those IPR-obeyed ones successfully, called Maximum Aromaticity Criterion (MARC), was shown by Garcia-Borràs and co-workers.[32] It is indicated that, in the case of endohedral metallofullerenes, both IPR isomers and non-IPR ones should be taken into consideration correspondingly. A very recent detailed investigation of the Gd_2C_{98} set revealed some remarkable significance on the thermodynamic stability of $Gd_2C_2@C_{96}$[33] instead of the previous IPR-violating one $Gd_2@C_2$(168785)-C_{98},[34] even though the latter one behaves much more stably than the lowest-energy IPR isomer $Gd_2@C_2$(230924)C_{98} in the system.

It has been shown on isomeric sets of fullerenes that potential energy itself cannot generally determine stability order at relative high temperatures for the entropic part of the Gibbs energy becomes essential.[35] As a result, the temperature-entropy effects by the Gibbs free energy function should been taken into consideration in order to determine the geometric structure of Gd_2C_{94}. Consequently, when the non-IPR isomers and temperature effect have been considered simultaneously, is C_2(153480)-C_{94} still a proper cage for a digadolinium encapsulated fullerene? If not, which structure does Gd_2C_{94}(II) possess, dimetallofullerene or carbide clusterfullerene?

To answer the above questions, a systematical theoretical study on both dimetallofullerenes $Gd_2@C_{94}$ and carbide clusterfullerenes $Gd_2C_2@C_{92}$ has been performed for the first time in this work. To the best of our knowledge, detailed structural studies on C_{94}-based EMFs are extremely lacking.[28] Indeed, only C_{94}-based monometallofullerene have been carefully studied. Interestingly, no matter what metal atom is encapsulated, the same C_{94}-C_{3v}(153493) cage[36,37] is chosen. The properties of dimetallofullerenes are incomparable with monometallofullerenes because of the different number of electrons transferred from metal atom(s) to carbon cages. Hence, our present study will provide a clearer sense of C_{94}-based and C_{92}-based EMFs.

COMPUTATIONAL DETAILS

Most of the IPR-violating fullerenes are regarded to be unstable and impossible of separation in the pristine fullerene form because of the quite large strain in adjacent pentagons.[38,39] Nevertheless, non-IPR fullerenes could be stabilized[17,20,34,40] by encapsulated metal ion(s) or metallocluster for the strong electronic interaction between metal ion(s) and adjacent pentagon pair(s) in carbon cages. Metal ions are mainly located upon the adjacent pentagon pairs in the non-IPR EMFs, so in general, the number of adjacent pentagon pairs is equal to the number of metal ions, while occasionally, exceptional cases may arise. For example, $Sc_2@C_{2v}$(7854)-C_{70}[20] has one pair of pentagon adjacency with no metal atom nearby. After all those factors have been considered, it is reasonable to choose 30 322 isomers of C_{94} cages and 22 082 isomers of C_{92} cages as appropriate candidates for Gd_2C_{94} structures. All of those isomers have no more than three adjacent pentagon pairs (number of pentagon adjacent pairs denoted by PA, namely, PA = 0−3).[41,42]

The 30 322 C_{94} isomers and the 21 374 C_{92} isomers[41] were primarily screened on the hexa-anion and tetra-anion state, respectively, at the AM1[43] level to evaluate the energetics for the C_{94} and C_{92} isomeric sets (see Tables S1 and S2 in the Supporting Information). Next, several lowest-energy anions were further optimized at the hybrid density functional B3LYP[44] level with the 6-31G(d) basis set (see Tables S3 and S4 in the Supporting Information). Then geometry optimizations of $Gd_2@C_{94}$ and $Gd_2C_2@C_{92}$ based on the optimization results of C_{94}^{6-} and C_{92}^{4-} were performed at the B3LYP/6-31G(d)∼CEP-31G level with the split-valence 6-31G(d) basis set for carbon atoms and CEP-31G[45] basis set with the corresponding pseudopotential for Gd atoms. To locate the lowest-energy arrangements, at least two more different positions of digadolinium atoms in a C_{94} cage or three more configurations, including linear and butterfly shapes, of the metal carbide cluster in a C_{92} cage have been taken into account. Since the gadolinium cation has an incomplete *f* shell ($4f^7$), the spin-unrestricted algorithms are used only. The results are listed in Table S5, Figures S1−S13, and Table S6 (Supporting Information), respectively. At last, several lowest-energies isomers in Table S6 were reoptimized at the B3LYP/6-311G(d)∼CEP-31G level of theory. All DFT calculations were carried out using the Gaussian 09 program package.[46]

Rotational−vibrational partition functions were calculated from the computed structural and vibrational data[47−49] at the B3LYP/3-21(d)∼CEP-31G level (though, only of the rigid rotator and harmonic oscillator quality and without any frequency scaling). Relative concentrations (molar fractions) w_i of i isomers can be expressed through the partition functions q_i and the ground-state energies $\Delta H^O_{0,i}$ by a compact formula

$$w_i = \frac{q_i \exp[-\Delta H^O_{0,i}/(RT)]}{\sum_{j=1}^{m} q_j \exp[-\Delta H^O_{0,j}/(RT)]} \quad (1)$$

dx.doi.org/10.1021/ic4022933 | Inorg. Chem. 2014, 53, 2012−2021

where R is the gas constant and T is the absolute temperature. Clearly enough, the conventional heats of formation at room temperature $\Delta H^{O}_{f,298}$ have to be converted to the heats of formation at the absolute zero temperature $\Delta H^{O}_{f,0}$. Chirality contributions, frequently ignored, must be also taken into account in eq 1 as its partition function q_i is doubled for an enantiomeric pair. In this way, the equilibrium concentrations can finally be evaluated, where the partial thermodynamic equilibrium is described by a set of equilibrium constants so that both enthalpy and entropy terms are considered accordingly. Noticeably, eq 1 is an exact relationship derived from the principle of equilibrium statistical thermodynamics, that is, from the standard Gibbs energies of isomers, and it is strongly temperature-dependent. All entropy contributions are evaluated through the isomeric partition functions.

RESULTS AND DISCUSSION

Relative energies and SOMO−LUMO gaps of several lowest-energy corresponding Gd_2C_{94} structures optimized at the B3LYP level are listed in Table 1. It is revealed that most of the energy superiority structures obey the IPR, and relative energies of those isomers with two or three adjacent pentagon pairs are found to be quite high, indicating the chemical instability (see Tables S1−S6 in the Supporting Information for details). Two isomers $Gd_2@C_2(153480)$-C_{94} and $Gd_2@C_2(153485)$-C_{94} possess the first and second lowest energies with a small difference of 2.0 kcal/mol. The $Gd_2C_2@D_3(126408)$-C_{92} is found to be the lowest-energy isomer among all $Gd_2C_2@C_{92}$ species. Meanwhile, among the whole Gd_2C_{94} system, the isomer $Gd_2C_2@D_3(126408)$-C_{92}, which has been separated and crystallized with Ni(OEP), possesses a relatively lower energy of 6.3 or 3.0 kcal/mol above the ground-state one at the B3LYP/6-31G(d)∼CEP-31G or more accurate B3LYP/6-311G(d)∼CEP-31G level, respectively. It is indicated that the stability order of EMFs cannot be completely determined by their relative energy. Accordingly, there is no evidence so far confirming that the $Gd_2@C_2(153480)$-C_{94} ought to be another stable isomer separated experimentally. At the same time, a smaller SOMO−LUMO gap (0.82 eV) of $Gd_2@C_2(153480)$-C_{94} indicates a low kinetic stability. More interestingly, three non-IPR structures and two more metallocarbide IPR structures have been exposed to possess not only relatively lower energies but also rather larger SOMO−LUMO gaps. Two aspects from both thermodynamic and kinetic viewpoints discussed above reveal that more elaborate identification should be taken theoretically into consideration to assist the experimental determination of other separated Gd_2C_{94} isomers. Therefore, it is obvious that relative stabilities of Gd_2C_{94} isomers based on the equilibrium statistical thermodynamics containing temperature effects should be examined to describe an overall thermodynamic stability of EMFs at relatively higher temperatures, especially for the fullerene-formation temperature region in a large number of previous investigations.[17,20,33,39,50]

The temperature−relative concentration curves of 10 Gd_2C_{94} isomers in a broad temperature region are presented in Figure 1. The $Gd_2@C_2(153480)$-C_{94}, which is the lowest-energy structure, must be prevailing at very low temperatures.

Table 1. Relative Energies and SOMO−LUMO Gaps of Gd_2C_{94} Isomers

		Gd_2C_{94}					
		B3LYP/6-31G(d)∼CEP-31G				B3LYP/6-311-G(d)∼CEP-31G	
sprial ID	IPR ID	PA	sym.[a]	ΔE[b]	gap[c]	ΔE[b]	gap[c]
C_{94}-153480	121	0	C_2	0.0	0.82	0.0	0.82
C_{94}-153485	126	0	C_2	2.0	0.76	2.2	0.76
C_{94}-153476	117	0	C_2	5.1	0.73	4.9	0.73
C_{94}-152345		1	C_s	10.9	0.79	11.0	0.79
C_{94}-153489	130	0	C_2	11.6	0.78	11.5	0.78
C_{94}-141346		1	C_1	12.9	1.48	13.1	1.47
C_{94}-153307		1	C_1	14.1	0.77	13.9	0.76
C_{92}-126408	85	0	D_3	6.3	1.68	3.0	1.67
C_{92}-126390	67	0	C_2	15.2	1.74	11.4	1.74
C_{92}-126387	64	0	C_1	10.2	1.60	6.6	1.61

[a]Symmetry of the original empty cage. [b]Relative energy (ΔE) units in kilocalories per mole. [c]SOMO−LUMO gap units in eV.

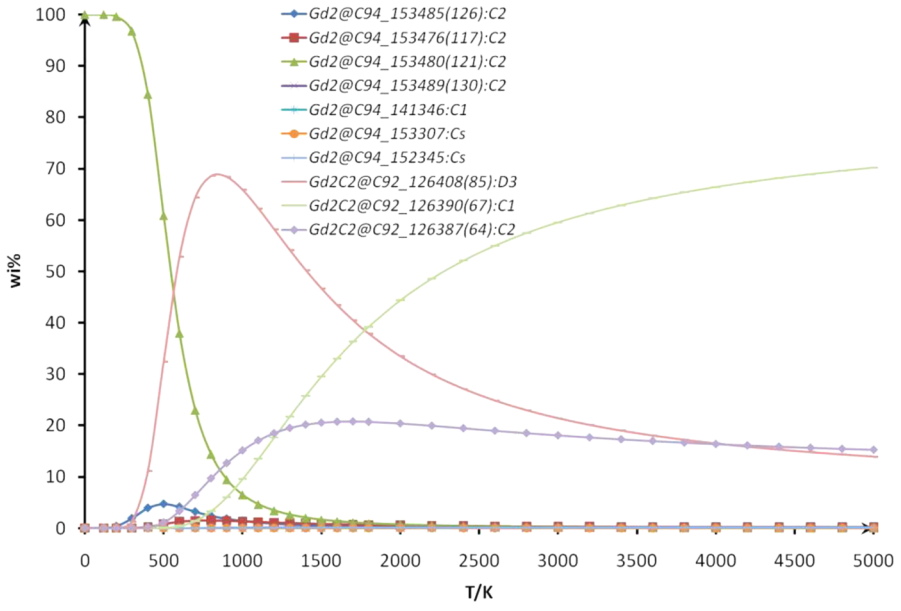

Figure 1. Relative concentrations of the Gd_2C_{94} isomers. The spiral numbers and IPR ID numbers (in parentheses) are labeled together in correspondence with experimental results.

dx.doi.org/10.1021/ic4022933 | Inorg. Chem. 2014, 53, 2012−2021

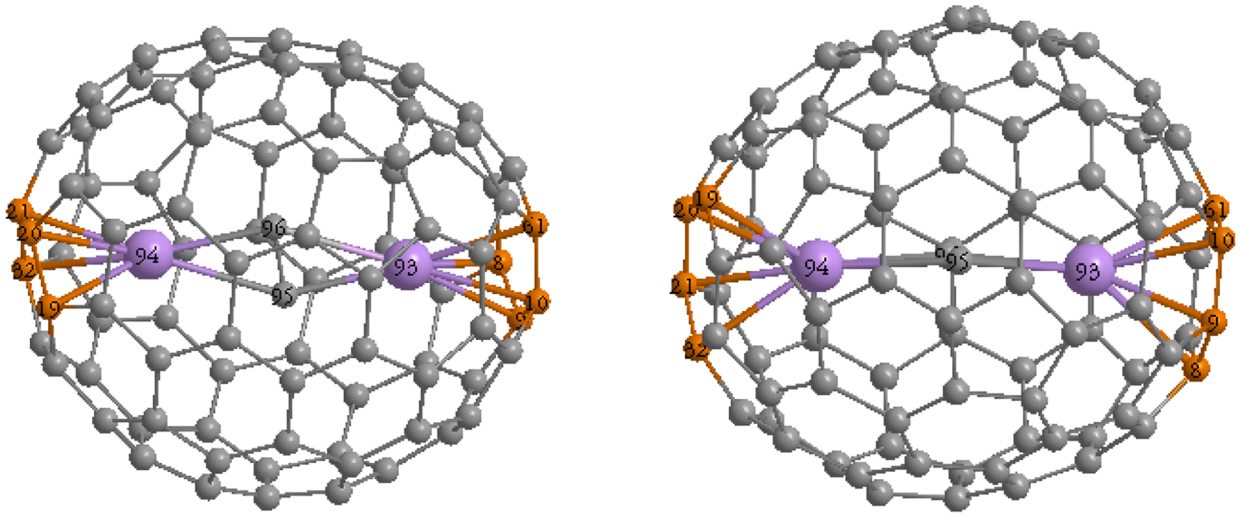

a. $Gd_2C_2@D_3(126408)$-C_{92}

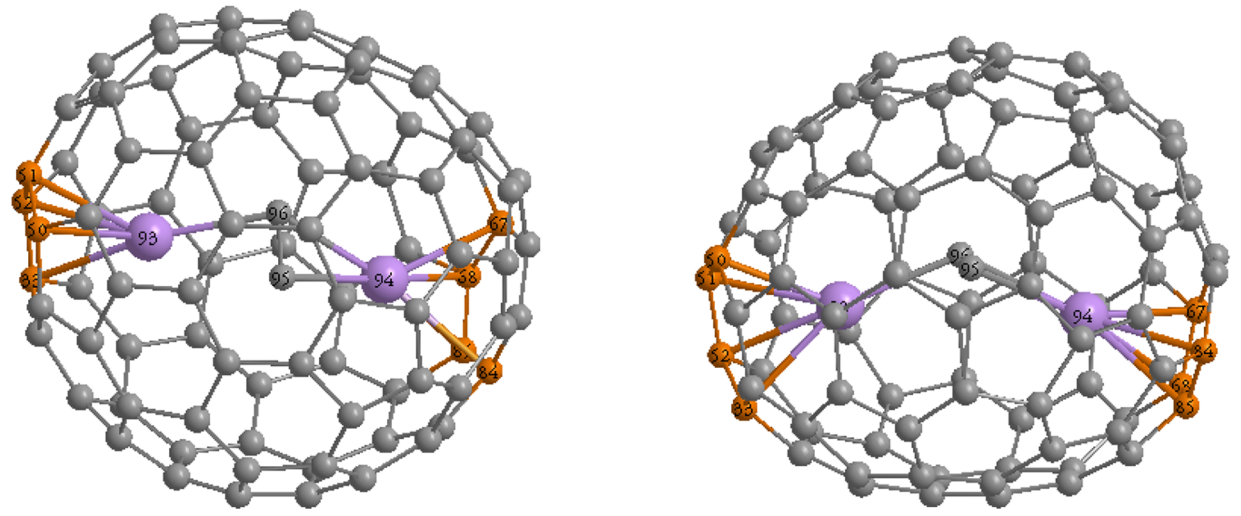

b. $Gd_2C_2@C_1(126390)$-C_{92}

Figure 2. Top (left) and side (right) views of the optimized structures (a) $Gd_2C_2@D_3(126408)$-C_{92} and (b) $Gd_2C_2@C_1(126390)$-C_{92}. In carbide structures, Gd atoms are colored violet and the carbon atoms in the cage connecting with the Gd atoms formally (shown by ChemBio 3D software) are colored orange.

Surprisingly, with the temperature increasing, its relative concentration declines rapidly and is surpassed by the isomer $Gd_2C_2@D_3(126408)$-C_{92} at about 500 K, and finally becomes very slight beyond 1000 K. At about 800 K, the relative concentration of $Gd_2C_2@D_3(126408)$-C_{92} ascends to its maximum yield of 69%, compared with a 14% fraction of the $Gd_2@C_2(153480)$-C_{94} species. After 800 K, although the fraction of $Gd_2C_2@D_3(126408)$-C_{92} decreases, it is still the most abundant structure within 1800 K. Noteworthy, with the temperature increase, the concentration of $Gd_2C_2@C_1(126390)$-C_{92} rises monotonously, and after 1800 K, the relative concentration of $Gd_2C_2@C_1(126390)$-C_{92} surpasses the fraction of $Gd_2C_2@D_3(126408)$-C_{92} and becomes the most important isomer. This trend lasts even when the temperature is as high as 5000 K. Additionally, another carbide clusterfullerene, $Gd_2C_2@C_2(126387)$-C_{92}, also has considerable concentrations in a board temperature region. At 1700 K, its concentration rises to the maximum of over 20%, and then with the continuous increase in the temperature, its mole fraction decreases tardily. Even at 5000 K, the relative concentration of $Gd_2C_2@C_2(126387)$-C_{92} can reach 13%. At the same time, other $Gd_2@C_{94}$ isomers, including $Gd_2@C_2(153485)$-C_{94}, of which the relative energy is only 2.0 kcal/mol higher than that of $Gd_2@C_2(153480)$-C_{94},[25] do not display any distinct stability throughout the whole temperature region. Consequently, the isomer $Gd_2C_2@D_3(126408)$-C_{92}, of which the single crystals have been produced, and $Gd_2C_2@C_1(126390)$-C_{92} species are proposed to be the most reasonable structures of the Gd_2C_{94} synthesized and isolated in the experiment. It is noteworthy that, to the best of our knowledge, $Gd_2C_2@C_1(126390)$-C_{92} has never been reported before. By the way, $Gd_2C_2@C_2(126387)$-C_{92} may also be detected and identified experimentally.

Figure 2 shows the top and side views of the optimized structures of $Gd_2C_2@D_3(126408)$-C_{92} and $Gd_2C_2@$

dx.doi.org/10.1021/ic4022933 | Inorg. Chem. 2014, 53, 2012−2021

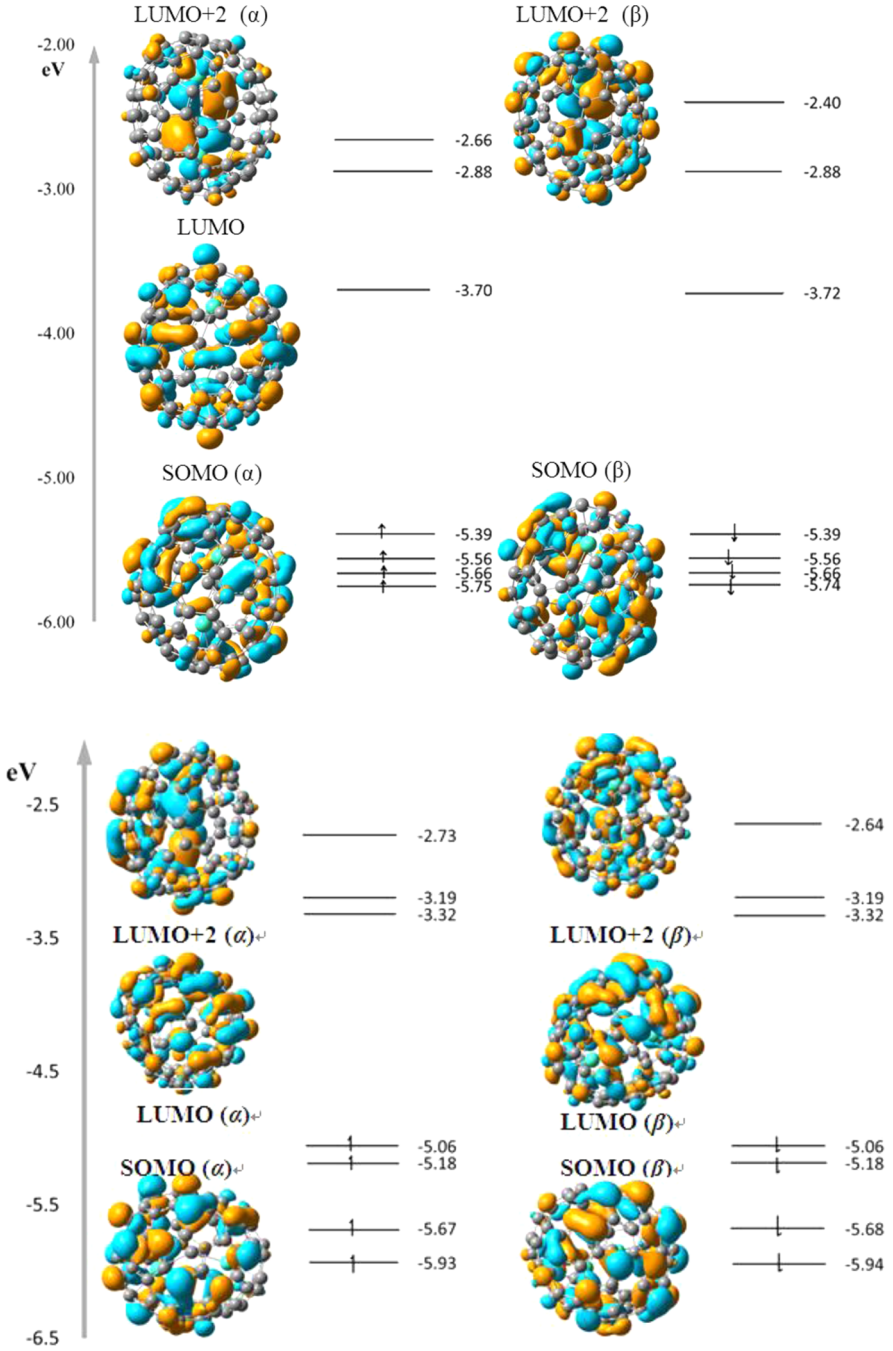

Figure 3. Main frontier molecular orbital diagrams of $Gd_2C_2@D_3(126408)$-C_{92} (top) and $Gd_2C_2@C_1(126390)$-C_{92} (bottom).

$C_1(126390)$-C_{92}, respectively. In the case of $Gd_2C_2@D_3(126408)$-C_{92}, the two Gd atoms of the metallocarbide cluster are coordinated to the C_3 axis with the distance of 4.805 Å, and the connecting line of the two carbon atoms of the cluster are perpendicular to the C_3 axis with the distance of 1.262 Å, which reveals that there is a triple bond between the two carbon atoms. For the carbide moiety, the Gd−C distances fall in the range of 2.371−2.612 Å. At the same time, the shortest distances of Gd93 and Gd94 to the C_{92} cage are 2.506 and 2.503 Å, respectively. The two coordinate sites of Gd atoms are located near two centers of hexagonal rings of the fullerene cage. Comparing with the empty cage, the cage is elongated along the C_3 axis after the cluster is encapsulated. In the cases of the empty $D_3(126408)$-C_{92} cage, the longest distance between two carbon atoms along the 3-fold axis is ~9.33 Å, whereas, after encapsulating the carbide, the distance increases to ~9.58 Å. All of the computational results are close to the previous experimental results presented by Yang and co-workers.[27]

As for another isomer $Gd_2C_2@C_1(126390)$-C_{92}, it is found that the average bonding angle of Gd−C−Gd in the cluster is obviously smaller than that in $Gd_2C_2@D_3(126408)$-C_{92}, and the distance of two Gd atoms slightly decreases to ~4.46 Å. Meanwhile, the distance between the C95 atom and the C96 one is 1.263 Å, which indicates that, although the configuration of the metallic carbide in the $Gd_2C_2@C_1(126390)$-C_{92} is different from the one in $Gd_2C_2@D_3(126408)$-C_{92}, a same C−C triple bond exists in this carbide structure. In the carbide

dx.doi.org/10.1021/ic4022933 | Inorg. Chem. 2014, 53, 2012−2021

moiety of $Gd_2C_2@C_1(126390)$-C_{92}, the bond lengths between Gd atoms and carbon atoms are from 2.415 to 2.625 Å with no obvious differences from the isomer discussed above. Similar to the $Gd_2C_2@D_3(126408)$-C_{92}, the two Gd atoms are also coordinated near two centers of hexagonal rings with the shortest distances of Gd93 and Gd94 to the C_{92} cage of 2.484 and 2.514 Å, respectively, which is also quite close to the situation described above.

Notably, the Gd_2C_2 clusters in two C_{92} cages with different symmetries present various shapes. Recently, two reports by Zhang et al.[51] and Nishimoto et al.[52] point out that fullerene cages containing a more linear Y-C-C-Y or Sc-C-C-Sc cluster are more stable than those containing the butterfly-shaped cluster. Herein, the linear $Gd_2C_2^{4+}$ and rhombic planar $Gd_2C_2^{4+}$ cations have been optimized with the B3LYP/6-31G(d)∼CEP-31G approach; accordingly related configurations and relative energies are achieved as depicted in Figure S14 and Table S7 (Supporting Information). Our DFT results show a good accordance with previous studies[51,52] that the free linear $Gd_2C_2^{4+}$ cation is 59.0 kcal/mol more stable than the free planar one. On the other hand, when the carbide cluster is encapsulated in a C_{92} fullerene, the limited inner cavity space of the cage leads to a cage compression,[51] resulting in a structural distortion of the Gd_2C_2 cluster. To investigate the influence of cluster distortion to the stability of the two isomers, single-point energy calculations of +4 charged Gd_2C_2 clusters derived from $D_3(126408)$ and $C_1(126390)$ cages were carried out, and the results are also listed in Table S7 (Supporting Information). Interestingly, the relative energy of +4 charged Gd_2C_2 derived from the $D_3(126408)$ cage is even lower than that of the free planar one; at the same time, the cluster derived from the $C_1(126390)$ cage has the highest relative energy among all four clusters. Consequently, the cluster derived from the $D_3(126408)$ cage is relatively relaxed. On the other hand, the steric strain of the cluster derived from the $C_1(126390)$ cage is much larger. Because of the better combination of both cage and inner cluster, the isomer $Gd_2C_2@D_3(126408)$-C_{92} presents a relatively lower energy compared with the $Gd_2C_2@C_1(126390)$-C_{92}.

When Yang et al. discussed the feasible structure of isomer II, they considered the $Gd_2C_2@C_1(126390)$-C_{92} structure, due to its relatively large (LUMO-3)−(LUMO-2) gap.[27] Regretfully, they did not insist just for a slightly higher relative energy than that of $Gd_2C_2@D_3(126408)$-C_{92} and $Gd_2@C_2$ (153480)-C_{94} structures. Thus, the relative energy itself cannot determine which isomers can be synthesized and separated. A quantum chemical calculation combined with statistical mechanics treatments should be utilized to study fullerenes theoretically, and the results could be accurate, which have been proven[17,20,34,40,50] by previous results. To date, besides $Gd_2C_2@D_3(126408)$-C_{92}, an appreciable quantity of C_{92}-based EMFs have been isolated and separated with none of them choosing the $C_1(126390)$-C_{92} cage, such as $Sm@C_s(126347)$-C_{92},[35] $Sm@C_1(126365)$-C_{92},[35] $Y_2C_2@D_3(126408)$-C_{92},[51,53] $Sm_2@D_3(126408)$-C_{92},[54] $La_3N@T(126409)$-C_{92},[55] and $La_3N@C_2(126359)$-C_{92}.[56] Consequently, it is for the first time that we find out an EMF with the $C_1(126390)$-C_{92} cage.

The main frontier molecular orbital diagrams of $Gd_2C_2@D_3(126408)$-C_{92} and $Gd_2C_2@C_1(126390)$-C_{92} with their singly occupied molecular orbitals (SOMO) and lowest unoccupied molecular orbitals (LUMO) are presented in Figure 3. Unlike two very large digadolinium EMFs $Gd_2@C_{98}$ reported recently,[34] the SOMO and LUMO of two $Gd_2C_2@C_{92}$ isomers investigated in this work are almost fully occupied by the molecular orbital from the C_{92} cage, as well as some other main frontier orbitals listed in Figures S15 and S16 of the Supporting Information. In both structures, the (LUMO+2) orbitals are most contributed from the encaged metal cluster, as shown in Figure 3. Because the frontier orbitals mainly distribute on the carbon cage in both structures, the electrochemical redox reactions should mainly occur on the fullerene cage, similar to the first non-IPR carbide cluster EMF, $Y_2C_2@C_{84}$.[17]

Although, in previous theoretical studies on carbide clusterfullerenes, a formal valence structure of $[M_2]^{6+}[C_2]^{2-}@[C_{2n}]^{4-}$ is usually considered,[17,21,30,57−63] numerous studies pointed out that the ionic model is oversimplified.[64] In fact, more than a decade ago, it was theoretically found that there is strong hybridization between the *d* valence orbitals of encapsulated metal atoms and the molecular orbitals of fullerene cage.[65,66] In 2009, an exhaustive study on metal−cage and inner cluster bonding was emerged by Popov et al.[64] By analyzing the bonding critical point (BCP) indicators, all types of bonding in EMFs exhibit a high degree of covalence. In our system, as mentioned above, although the C95−C96 distance of either $Gd_2C_2@D_3(126408)$-C_{92} or $Gd_2C_2@C_1(126390)$-C_{92} is about 1.26 Å, which is equal to the C−C bond length of the typical −2 charged C_2 unit in Li_2C_2 or CaC_2 (∼1.26 Å),[67] relatively substantial orbital overlaps between metallic atomic orbitals and cage orbitals have been found from the *β*-(HOMO-10) and *β*-(HOMO-11) orbitals of both $Gd_2C_2@D_3(126408)$-C_{92} and $Gd_2C_2@C_1(126390)$-C_{92} isomers (see Figures S17 and S18, Supporting Information, for details). As a result, both covalent and ionic interactions between the cluster and the cage may coexist.

To obtain more detailed information on cluster−cage interactions, Mulliken charge distributions, natural bond orbital (NBO) population analysis, and Mayer bond order[68−70] of $Gd_2C_2@D_3(126408)$-C_{92} and $Gd_2C_2@C_1(126390)$-C_{92} have been employed. The Mulliken charge distributions of $Gd_2C_2@D_3(126408)$-C_{92} and $Gd_2C_2@C_1(126390)$-C_{92} are depicted in Figure 4. For both structures, two gadolinium atoms present

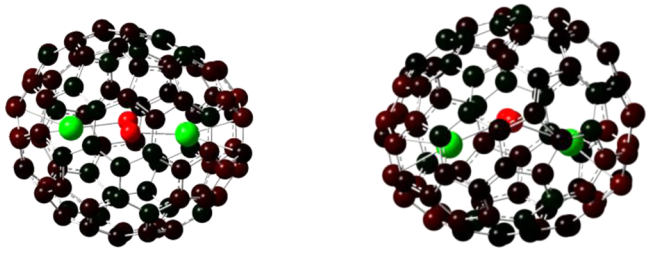

Figure 4. Mulliken charge distribution of $Gd_2C_2@D_3(126408)$-C_{92} (left) and $Gd_2C_2@C_1(126390)$-C_{92} (right).

the positive charge. Meanwhile, although all carbon atoms are negatively charged, they can be divided into two types, that is, carbons in the carbide cluster (i.e., C95 and C96, Type A) and carbons in the cage (Type B). As shown in Figure 4, the charge of Type A is much more negative than that of Type B. At the same time, because both of the two carbon cages investigated here obey the IPR, the phenomenon of "charge concentration" is less apparent than that of $Gd_2@C_1(16875)$-C_{98}, of which the cage is a IPR-violating one. For those reasons, it seems that the charge distribution of the different C atoms in the cage is similar. On the other hand, if the carbon atoms of Type B were

dx.doi.org/10.1021/ic4022933 | *Inorg. Chem.* 2014, 53, 2012−2021

Table 2. Natural Electron Configuration Populations of Gd Atoms and Carbon Atoms in Gd_2C_2@C_1(126390)-C_{92}, Gd_2C_2@D_3(126408)-C_{92}, and +4 Charged Gd_2C_2 Cluster from Gd_2C_2@C_1(126390)-C_{92} and Gd_2C_2@D_3(126408)-C_{92} Molecules, Respectively, and Optimized Structure of Neutral Gd_2C_2 Molecule

		charge	populations
Gd_2C_2@C_1(126390)-C_{92}	Gd93	1.65348	$4f^{7.02}5d^{0.88}6s^{0.15}6p^{0.31}6d^{0.01}7p^{0.01}$
	Gd94	1.65875	$4f^{7.02}5d^{0.86}6s^{0.16}6p^{0.31}6d^{0.01}7p^{0.01}$
	C95	−0.46158	$2s^{1.35}2p^{3.08}3p^{0.02}3d^{0.01}$
	C96	−0.55737	$2s^{1.33}2p^{3.20}3p^{0.02}3d^{0.01}$
Gd_2C_2_from 126390_+4 charged	Gd1	2.68746	$4f^{7.01}5d^{0.21}6s^{0.08}6p^{0.02}$
	Gd2	2.66831	$4f^{7.01}5d^{0.22}6s^{0.09}6p^{0.02}$
	C1	−0.57080	$2s^{1.50}2p^{3.04}3p^{0.02}3d^{0.01}$
	C2	−0.78497	$2s^{1.50}2p^{3.26}3p^{0.02}3d^{0.01}$
Gd_2C_2@D_3(126408)-C_{92}	Gd93	1.67891	$4f^{7.02}5d^{0.86}6s^{0.15}6p^{0.31}6d^{0.01}7p^{0.01}$
	Gd94	1.68482	$4f^{7.02}5d^{0.86}6s^{0.15}6p^{0.30}6d^{0.01}7p^{0.01}$
	C95	−0.50832	$2s^{1.34}2p^{3.14}3p^{0.02}3d^{0.01}$
	C96	−0.53891	$2s^{1.33}2p^{3.18}3p^{0.02}3d^{0.01}$
Gd_2C_2_from 126408_+4 charged	Gd1	2.68240	$4f^{7.01}5d^{0.25}6s^{0.06}6p^{0.02}$
	Gd2	2.68240	$4f^{7.01}5d^{0.25}6s^{0.06}6p^{0.02}$
	C1	−0.68240	$2s^{1.62}2p^{3.04}3p^{0.02}3d^{0.01}$
	C2	−0.68240	$2s^{1.62}2p^{3.04}3p^{0.02}3d^{0.01}$
Gd_2C_2_neutral	Gd1	0.99764	$4f^{7.01}5d^{0.86}6s^{1.08}6p^{0.10}$
	Gd2	0.99764	$4f^{7.01}5d^{0.86}6s^{1.08}6p^{0.10}$
	C1	−0.99764	$2s^{1.45}2p^{3.53}3p^{0.02}3d^{0.01}$
	C2	−0.99764	$2s^{1.45}2p^{3.53}3p^{0.02}3d^{0.01}$

Table 3. Mayer Bond Order between Gd Atoms and Carbon Atoms Bonding Formally Shown by GaussView 5.0

			alpha	beta	total			alpha	beta	total
Gd_2C_2@C_1(126390)-C_{92}	Gd93	C33	0.0999	0.0904	0.188	Gd94	C67	0.103	0.0931	0.194
		C50	0.113	0.102	0.213		C68	0.0840	0.0768	0.160
		C51	0.0909	0.0830	0.172		C84	0.100	0.0903	0.189
		C52	0.0970	0.0888	0.184		C85	0.102	0.0932	0.193
		C95	0.198	0.190	0.385		C95	0.315	0.295	0.608
		C96	0.316	0.294	0.607		C96	0.241	0.228	0.467
Gd_2C_2@D_3(126408)-C_{92}	Gd93	C8	0.0962	0.0868	0.181	Gd94	C19	0.101	0.0907	0.190
		C9	0.104	0.0942	0.196		C20	0.103	0.0931	0.194
		C10	0.104	0.0818	0.170		C21	0.0875	0.0803	0.167
		C61	0.101	0.0906	0.189		C32	0.0994	0.0897	0.187
		C95	0.329	0.307	0.633		C95	0.202	0.193	0.392
		C96	0.211	0.201	0.410		C96	0.336	0.313	0.646

further considered, they can be divided into carbons belonging to a five-membered ring (i.e., [5, 6]-carbon) and a six-membered ring (i.e., [6, 6]-carbon), respectively. Figure 4 shows that the charge distributed on [5, 6]-carbons is more negative than that on [6, 6]-carbons. Although the previous studies indicate that five-membered rings accumulated the charge transfer from the metal cluster, our finding here reveals that the carbon atoms in both five-membered and six-membered rings can accumulate the charge transfer from the metal cluster, and it seems that the carbon atoms in the five membered rings are willing to accept more charges.

Natural electron configuration analyses of Gd_2C_2@D_3(126408)-C_{92}, Gd_2C_2@C_1(126390)-C_{92}, and +4 charged Gd_2C_2 clusters from Gd_2C_2@D_3(126408)-C_{92} and Gd_2C_2@C_1(126390)-C_{92} molecules are also performed, respectively, and the optimized structure of the neutral Gd_2C_2 cluster, as shown in Table 2. The neutral Gd_2C_2 cluster was optimized at the B3LYP/6-31G(d)~CEP-31G level, and its structure is depicted in Figure S19 in the Supporting Information. The atomic populations for the neutral Gd_2C_2 cluster shows that it is a polar molecule with negative charges localized on the two C atoms (−1.0 *e*) and positive charges on each Gd of +1.0 *e*. Taking the optimized Gd_2C_2 neutral cluster as a reference, the Gd_2C_2 encapsulation into D_3(126408)-C_{92} and C_1(126390)-C_{92} cages will induce a lowering from 0.92 to 0.93 electrons in the 6*s* orbital of each Gd atoms. However, the population of 4*f* and 5*d* orbitals does not have significant changes in two structures, while the population of 6*p* orbitals slightly increases by 0.20−0.21 electrons, indicating a consequence of the back-donation from cage orbitals to the metallic orbitals. In total, the charges on the Gd in the Gd_2C_2@D_3(126408)-C_{92} and Gd_2C_2@C_1(126390)-C_{92} molecules are +1.68 and +1.65 *e*, respectively. All of the charges on the Gd atoms in the endohedral fullerenes are positive, but far from +2.66 to +2.68 *e*, the positive charges of the metal ion in the +4 charged free metallic cluster derived from Gd_2C_2@D_3(126408)-C_{92} and Gd_2C_2@C_1(126390)-C_{92}, respectively. The charge transfers between the inner cluster and the carbon cage of Gd_2C_2@D_3(126408)-C_{92} and Gd_2C_2@C_1(126390)-C_{92} are 2.31and 2.29 *e*, respectively, both of which are less than the ideal 4.0 *e*. As a result, the ionic model can partially describe the interaction between metal and carbon atoms only.

dx.doi.org/10.1021/ic4022933 | *Inorg. Chem.* 2014, 53, 2012−2021

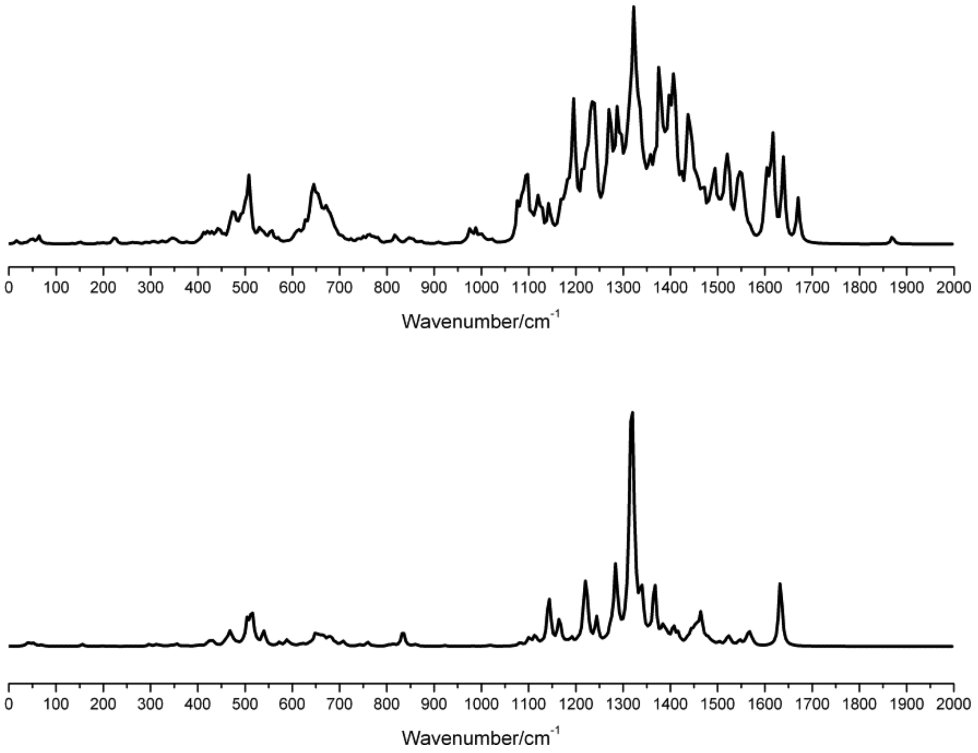

Figure 5. Simulated IR spectra of $Gd_2C_2@D_3(126408)$-C_{92} (top) and $Gd_2C_2@C_1(126390)$-C_{92} (bottom).

To gain a deeper insight into the covalent bonding, Mayer bond orders were examined by using the MUTIWFN 3.2[71] program, and the results are collected in Table 3. In general, the Mayer bond order of the two isomers has similar regularity; that is, the Mayer bond order between gadolinium atoms and one of the carbon atoms in the cluster (i.e., Gd93−C96 and Gd94−C95) is over 0.6, which indicates that the covalent interaction cannot be ignored. At the same time, the Mayer bond order between gadolinium atoms and carbon atoms in the cage is much smaller, revealing that, compared with the covalent interactions, the ionic interactions between the carbide cluster and carbon cage are much more important. For the isomers $Gd_2C_2@D_3(126408)$-C_{92} and $Gd_2C_2@C_1(126390)$-C_{92}, the largest Mayer bond orders between a gadolinium atom and a carbon atom in the cage are 0.196 (Gd93−C9) and 0.213 (G93−C50), respectively. Therefore, the covalent interactions between Gd and the carbon atom in the cage of $Gd_2C_2@C_1(126390)$-C_{92} is a little more significant than that of $Gd_2C_2@D_3(126408)$-C_{92}, and that may be the reason why the charge transfer between the inner cluster and the carbon cage of $Gd_2C_2@C_1(126390)$-C_{92} is a bit smaller. According to the discussion above, we suggest that the ionic model should be expressed as $[Gd_2C_2]^{n+}C_{92}^{n-}$ rather than $[Gd_2]^{6+}[C_2]^{n-}$-$[C_{92}]^{(6-n)-}$ as a consequence of the existence of the covalent interactions between Gd and carbon atoms in the cluster.

The high stability of $Gd_2C_2@D_3(126408)$-C_{92} and $Gd_2C_2@C_1(126390)$-C_{92} can also be explained in terms of their frontier molecular orbital. As shown in Table1, all of the dimetal isomers have a small SOMO−LUMO gap, and this demostrates that all of the C_{94} isomers are kinetically unstable for their electrons can jump easily. Oppositely, three C_{92}-based carbide cluster fullerenes possess a relatively large SOMO−LUMO gap, especially $Gd_2C_2@C_1(126390)$-C_{92} and $Gd_2C_2@D_3(126408)$-C_{92}, which have the first and the second largest SOMO−LUMO gaps, and consequently have enough higher kinetic stability to be separated.

Since the infrared (IR) spectra are very sensitive to the molecular structure of EMFs,[39] not only structural confirmation but also some interesting information on encapsulated metalloclusters can be obtained from IR spectra. Therefore, IR spectra of $Gd_2C_2@D_3(126408)$-C_{92} and $Gd_2C_2@C_1(126390)$-C_{92} were simulated theoretically by harmonic vibrational analyses at the B3LYP/3-21G*∼CEP-31G level of theory.

The IR spectra are depicted in Figure 5, which are useful for further experimental characterization. It is clear that both of the spectra can be mainly divided into three regions. The lowest region from 0 to 200 cm^{-1}, which is attributed to the frustrated translation and rotation of the " Gd_2C_2" cluster, is much weaker. It can be explained from the large mass of metallic ions of the cluster that those modes present rather low frequencies.[72] The second region (200−1100 cm^{-1}) corresponds to a cage " breathing " mode, and the third one (1100−2000 cm^{-1}) corresponds to a C−C stretching mode of the fullerene cage. Specially, in the spectrum of $Gd_2C_2@C_1(126390)$-C_{92}, there is a very weak absorption peak at 1870 cm^{-1}. It is the stretching vibration of the central "C_2" perssad. Analogously, for the central "C_2" perssad in $Gd_2C_2@D_3(126408)$-C_{92}, its C−C stretching frequency is 1842 cm^{-1}. Unfortunately, the absorption peak is too weak to visualize in the figure. Unlike the case of $Sc_4C_2@C_{80}$,[73] their signals appear at the maximum absorption wavenumber and are not merged with the nearby signals arising from vibrations of carbon cages. Nevertheless, the absorption intensity of them is too low to be a fingerprint for characterization of $Gd_2C_2@C_{92}$. Fortunately, both the second and the third region exhibit some other differences between $Gd_2C_2@D_3(126408)$-C_{92} and $Gd_2C_2@C_1(126390)$-C_{92}, which is helpful to identify the two molecules. In the second region, $Gd_2C_2@D_3(126408)$-C_{92} displays only

dx.doi.org/10.1021/ic4022933 | Inorg. Chem. 2014, 53, 2012−2021

one weak peak at ~500 cm^{-1}, whereas $Gd_2C_2@C_1(126390)$-C_{92} shows two higher peaks at ~500 and ~650 cm^{-1} respectively. Meanwhile, one distinct sharp absorption peak at 1320 cm^{-1} for isomer $Gd_2C_2@D_3(126408)$-C_{92} is presented, in contrast to the much lower absorption bands exhibiting at the same region for another C_{92}-based carbide cluster fullerene.

CONCLUSIONS

By means of the density functional theory technique, a theoretical investigation has been performed on the digadolinium-containing endohedral metallofullerene Gd_2C_{94}, of which both dimetallofullerenes and carbide clusterfullerene structures have been taken into consideration. Unfortunately, although the isomer $Gd_2@C_2(153480)$-C_{94}, predicted as another proper Gd_2C_{94} isomer in the previous experiment, possesses the lowest relative energy, it is not thermodynamically prevailing at elevated temperatures. Compared with two lowest-energy isomers, $Gd_2@C_2(153480)$-C_{94} and $Gd_2@C_2(153485)$-C_{94}, the relative energies of three carbide clusterfullerene isomers, $Gd_2C_2@D_3(126408)$-C_{92}, $Gd_2C_2@C_2(126387)$-C_{92}, and $Gd_2C_2@C_1(126390)$-C_{92}, are somewhat higher, but owning much larger SOMO−LUMO gaps, which indicates relatively higher chemical stabilities. On the basis of statistical thermodynamics theory, temperature effects have also been taken into account to clarify relative stabilities at the temperature region of fullerene formation. The results indicate that two carbide clusterfullerene isomers $Gd_2C_2@D_3(126408)$-C_{92} and $Gd_2C_2@C_1(126390)$-C_{92}, rather than two dimetallofullerenes $Gd_2@C_2(153480)$-C_{94} and $Gd_2@C_2(153485)$-C_{94}, should be the most thermodynamically superior isomers for Gd_2C_{94} species. The $Gd_2C_2@C_1(126390)$-C_{92}, which has never been reported before, is predicted to be that structure Gd_2C_{94}(II) synthesized experimentally. The analyses of frontier molecular orbitals, Mulliken charge distribution, NBO population, and Mayer bond order reveal that both covalent and ionic interactions coexist between Gd atoms and carbon atoms in the cluster, and the ionic model should be expressed as $[Gd_2C_2]^{n+}C_{92}^{n-}$ rather than $[Gd_2]^{6+}[C_2]^{n-}[C_{92}]^{(6-n)-}$. Additionally, simulated IR spectra of $Gd_2C_2@D_3(126408)$-C_{92} and $Gd_2C_2@C_1(126390)$-C_{92} show some different absorption bands in a broad region, which is helpful to further experimental identification of $Gd_2C_2@C_{92}$. The present work could enrich the C_{92}-based endohedral metallofullerenes and supply some valuable assistance for the experimental characterizations.

ASSOCIATED CONTENT

Supporting Information

Relative energies of C_{92} and C_{94} at tetra-anion and hexa-anion states, respectively, and Cartesian coordinates of two major isomers $Gd_2C_2@C_{92}$ optimized at the B3LYP level. This material is available free of charge via the Internet at http://pubs.acs.org.

AUTHOR INFORMATION

Corresponding Author

*E-mail: xzhao@mail.xjtu.edu.cn.

Notes

The authors declare no competing financial interest.

ACKNOWLEDGMENTS

This work has been financially supported by the National Natural Science Foundation of China (No. 21171138), the National Key Basic Research Program of China (Nos. 2011CB209404, 2012CB720904), and the Specialized Research Fund for the Doctoral Program of Higher Education of China (SRFDP No. 20130201110033).

REFERENCES

(1) Chai, Y.; Guo, T.; Jin, C.; Haufler, R. E.; Chibante, L. P. F.; Fure, J.; Wang, L.; Alford, J. M.; Smalley, R. E. *J. Phys. Chem.* **1991**, *95*, 7564.
(2) Maeda, Y.; Tsuchiya, T.; Lu, X.; Takano, Y.; Akasaka, T.; Nagase, S. *Nanoscale* **2011**, *3*, 2421.
(3) Zhong, X.; Yuan, R.; Chai, Y. *Chem. Commun.* **2012**, *48*, 597.
(4) Rodríguez-Fortea, A.; Balch, A. L.; Poblet, J. M. *Chem. Soc. Rev.* **2011**, *40*, 3551.
(5) Tzirakis, M. D.; Orfanopoulos, M. *Chem. Rev.* **2013**, *113*, 5262.
(6) Osuna, S.; Swart, M.; Sola, M. *Phys. Chem. Chem. Phys.* **2011**, *13*, 3585.
(7) Rivera-Nazario, D. M.; Pinzon, J. R.; Stevenson, S.; Echegoyen, L. A. *J. Phys. Org. Chem.* **2013**, *26*, 194.
(8) Wilson, L. J.; Cagle, D. W.; Thrash, T. P.; Kennel, S. J.; Mirzadeh, S.; Alford, J. M.; Ehrhardt, G. J. *Coord. Chem. Rev.* **1999**, *192*, 199.
(9) Akasaka, T., Nagase, S., Eds. *Endofullerenes: A New Family of Carbon Clusters*; Developments in Fullerene Science, Vol. 3; Kluwer: Dordrecht, 2002.
(10) Chaur, M. N.; Melin, F.; Ortiz, A. L.; Echegoyen, L. *Angew. Chem., Int. Ed.* **2009**, *48*, 7514.
(11) Akasaka, T., Wudl, F., Nagase, S., Eds. *Chemistry of Nanocarbons*; Wiley-Blackwell: London, 2010.
(12) Lu, X.; Akasaka, T.; Nagase, S. *Chem. Commun.* **2011**, *47*, 5942.
(13) Shinohara, H. *Rep. Prog. Phys.* **2000**, *63*, 843.
(14) Wang, C.-R.; Kai, T.; Tomiyama, T.; Yoshida, T.; Kobayashi, Y.; Nishibori, E.; Takata, M.; Sakata, M.; Shinohara, H. *Angew. Chem., Int. Ed.* **2001**, *40*, 397.
(15) Kurihara, H.; Lu, X.; Iiduka, Y.; Nikawa, H.; Hachiya, M.; Mizorogi, N.; Slanina, Z.; Tsuchiya, T.; Nagase, S.; Akasaka, T. *Inorg. Chem.* **2012**, *51*, 746.
(16) Chen, C.-H.; Yeh, W.-Y.; Liu, Y.-H.; Lee, G.-H. *Angew. Chem., Int. Ed.* **2012**, *51*, 13046.
(17) Yang, T.; Zhao, X.; Li, S.-T.; Nagase, S. *Inorg. Chem.* **2012**, *51*, 11223.
(18) Kroto, H. W. *Nature* **1987**, *329*, 529.
(19) Shi, Z.-Q.; Wu, X.; Wang, C.-R.; Lu, X.; Shinohara, H. *Angew. Chem., Int. Ed.* **2006**, *45*, 2107.
(20) Zheng, H.; Zhao, X.; Wang, W.-W.; Yang, T.; Nagase, S. *J. Chem. Phys.* **2012**, *137*, 014308.
(21) Cao, B. P.; Hasegawa, M.; Okada, K.; Tomiyama, T.; Okazaki, T.; Suenaga, K.; Shinohara, H. *J. Am. Chem. Soc.* **2001**, *123*, 9679.
(22) Tan, K.; Lu, X. *Chem. Commun.* **2005**, 4444.
(23) Yumura, T.; Sato, Y.; Suenaga, K.; Iijima, S. *J. Phys. Chem. B* **2005**, *109*, 20251.
(24) (a) Kurihara, H.; Lu, X.; Iiduka, Y.; Mizorogi, N.; Slanina, Z.; Tsuchiya, T.; Akasaka, T.; Nagase, S. *J. Am. Chem. Soc.* **2011**, *133*, 2382. (b) Kurihara, H.; Lu, X.; Iiduka, Y.; Nikawa, H.; Mizorogi, N.; Slanina, Z.; Tsuchiya, T.; Nagase, S.; Akasaka, T. *J. Am. Chem. Soc.* **2012**, *134*, 3139.
(25) Lu, X.; Nakajima, K.; Iiduka, Y.; Nikawa, H.; Mizorogi, N.; Slanina, Z.; Tsuchiya, T.; Nagase, S.; Akasaka, T. *J. Am. Chem. Soc.* **2011**, *133*, 19553.
(26) Iiduka, Y.; Wakahara, T.; Nakajima, K.; Tsuchiya, T.; Nakahodo, T.; Maeda, Y.; Akasaka, T.; Mizorogi, N.; Nagase, S. *Chem. Commun.* **2006**, 2057.
(27) Yang, H.; Lu, C.; Liu, Z.; Jin, H.; Che, Y.; Olmstead, M. M.; Balch, A. L. *J. Am. Chem. Soc.* **2008**, *130*, 17296.
(28) Popov, A. A.; Yang, S.; Dunsch, L. *Chem. Rev.* **2013**, *113*, 5989.
(29) Popov, A. A.; Dunsch, L. *J. Am. Chem. Soc.* **2007**, *129*, 11835.
(30) Valencia, R.; Rodríguez-Fortea, A.; Poblet, J. M. *J. Phys. Chem. A* **2008**, *112*, 4550.
(31) Yang, T.; Zhao, X.; Nagase, S. *Phys. Chem. Chem. Phys.* **2011**, *13*, 5034.

(32) Garcia-Borràs, M.; Osuna, S.; Swart, M.; Luis, J. M.; Solà, M. *Angew. Chem., Int. Ed.* **2013**, *52*, 9275.
(33) Zheng, H.; Zhao, X.; Wang, W. W.; Dang, J. S.; Nagase, S. *J. Phys. Chem. C* **2013**, *117*, 25195.
(34) Zhao, X.; Gao, W.-Y.; Yang, T.; Zheng, J.-J.; Li, L.-S.; He, L.; Cao, R.-J.; Nagase, S. *Inorg. Chem.* **2012**, *51*, 2039.
(35) Slanina, Z.; UhlíŘ, F.; Zhao, X.; Ōsawa, E. *J. Chem. Phys.* **2000**, *113*, 4933.
(36) Che, Y.; Yang, H.; Wang, Z.; Jin, H.; Liu, Z.; Lu, C.; Zuo, T.; Dorn, H. C.; Beavers, C. M.; Olmstead, M. M.; Balch, A. L. *Inorg. Chem.* **2009**, *48*, 6004.
(37) Jin, H.; Yang, H.; Yu, M.; Liu, Z.; Beavers, C. M.; Olmstead, M. M.; Balch, A. L. *J. Am. Chem. Soc.* **2012**, *134*, 10933.
(38) Albertazzi, E.; Domene, C.; Fowler, P. W.; Heine, T.; Seifert, G.; Van Alsenoy, C.; Zerbetto, F. *Phys. Chem. Chem. Phys.* **1999**, *1*, 2913.
(39) Campbell, E. E. B.; Fowler, P. W.; Mitchell, D.; Zerbetto, F. *Chem. Phys. Lett.* **1996**, *250*, 544.
(40) Yang, T.; Zhao, X.; Nagase, S. *Chem.—Eur. J.* **2013**, *19*, 2649.
(41) Fowler, P. W.; Manoloupoulos, D. E. *An Atlas of Fullerenes*; Oxford University Press: Oxford, U.K., 1995.
(42) Zhao, X.; Slanina, Z. *J. Mol. Struct.: THEOCHEM* **2003**, *636*, 195.
(43) Dewar, M. J. S.; Zoebisch, E.; Healy, E. F.; Stewart, J. J. P. *J. Am. Chem. Soc.* **1985**, *107*, 3902.
(44) (a) Becke, A. D. *Phys. Rev. A* **1988**, *38*, 3098. (b) Becke, A. D. *J. Chem. Phys.* **1993**, *98*, 5648. (c) Lee, C.; Yang, W.; Parr, R. G. *Phys. Rev. B: Condens. Matter Mater. Phys.* **1988**, *37*, 785.
(45) Cundari, T. R; Stevens, W. J. *J. Chem. Phys.* **1993**, *98*, 5555.
(46) Frisch, M. J.; Trucks, G. W.; Schlegel, H. B.; Scuseria, G. E.; Robb, M. A.; Cheeseman, J. R.; Scalmani, G.; Barone, V.; Mennucci, B.; Petersson, G. A.; Nakatsuji, H.; Caricato, M.; Li, X.; Hratchian, H. P.; Izmaylov, A. F.; Bloino, J.; Zheng, G.; Sonnenberg, J. L.; Hada, M.; Ehara, M.; Toyota, K.; Fukuda, R.; Hasegawa, J.; Ishida, M.; Nakajima, T.; Honda, Y.; Kitao, O.; Nakai, H.; Vreven, T.; Montgomery, J. A., Jr.; Peralta, J. E.; Ogliaro, F.; Bearpark, M.; Heyd, J. J.; Brothers, E.; Kudin, K. N.; Staroverov, V. N.; Kobayashi, R.; Normand, J.; Raghavachari, K.; Rendell, A. J.; Burant, C.; Iyengar, S. S.; Tomasi, J.; Cossi, M.; Rega, N.; Millam, J. M.; Klene, M.; Knox, J. E.; Cross, J. B.; Bakken, V.; Adamo, C.; Jaramillo, J.; Gomperts, R.; Stratmann, R. E.; Yazyev, O.; Austin, A. J.; Cammi, R.; Pomelli, C.; Ochterski, J. W.; Martin, R. L.; Morokuma, K.; Zakrzewski, V. G.; Voth, G. A.; Salvador, P.; Dannenberg, J. J.; Dapprich, S.; Daniels, A. D.; Farkas, Ö.; Foresman, J. B.; Ortiz, J. V.; Cioslowski, J.; Fox, D. J. *Gaussian 09*, Revision A.01; Gaussian, Inc.: Wallingford, CT, 2009.
(47) Slanina, Z. *Int. Rev. Phys. Chem.* **1987**, *6*, 251.
(48) Slanina, Z.; Lee, S.-L.; Adamowicz, F. U. L.; Nagase, S. *Theor. Chem. Acc.* **2007**, *117*, 315.
(49) Zhao, X. *J. Phys. Chem. B* **2005**, *109*, 5267.
(50) Zheng, H.; Zhao, X.; Ren, T.; Wang, W.-W. *Nanoscale* **2012**, *4*, 4530.
(51) Zhang, J.; Fuhrer, T.; Fu, W.; Ge, J.; Bearden, D. W.; Dallas, J. L.; Duchamp, J. C.; Walker, K. L.; Champion, H.; Azurmendi, H. F.; Harich, K.; Dorn, H. C. *J. Am. Chem. Soc.* **2012**, *134*, 8487.
(52) Nishimoto, Y.; Wang, Z.; Morokuma, K.; Irle, S. *Phys. Status Solidi B* **2012**, *249*, 324.
(53) Burke, B. G.; Chan, J.; Williams, K. A.; Fuhrer, T.; Fu, W.; Dorn, H. C.; Puretzky, A. A.; Geohegan, D. B. *Phys. Rev. B* **2011**, *83*, 115457.
(54) Yang, H.; Jin, H.; Hong, B.; Liu, Z.; Beavers, C. M.; Zhen, H.; Wang, Z.; Mercado, B. Q.; Olmstead, M. M.; Balch, A. L. *J. Am. Chem. Soc.* **2011**, *133*, 16911.
(55) Chaur, M. N.; Valencia, R.; Rodriguez-Fortea, A.; Poblet, J. M.; Echegoyen, L. *Angew. Chem., Int. Ed.* **2009**, *48*, 1425.
(56) Zheng, J. J.; Zhao, X.; Dang, J. S.; Chen, Y. M.; Xu, Q.; Wang, W. W. *Chem. Phys. Lett.* **2011**, *514*, 104.
(57) Inoue, T.; Tomiyama, T.; Sugai, T.; Okasaki, T.; Suematsu, T.; Fujii, N.; Utsumi, H.; Nojima, K.; Shinohara, H. *J. Phys. Chem. B* **2004**, *108*, 7573.
(58) Iiduka, Y.; Wakahara, T.; Nakajima, K.; Tsuchiya, T.; Nakahodo, T.; Maeda, Y.; Akasaka, T.; Mizorogi, N.; Nagase, S. *Chem. Commun.* **2006**, 2057.
(59) Iiduka, Y.; Wakahara, T.; Nakajima, K.; Nakahodo, T.; Tsuchiya, T.; Maeda, Y.; Akasaka, T.; Yoza, K.; Liu, M. T. H.; Mizorogi, N.; Nagase, S. *Angew. Chem., Int. Ed.* **2007**, *46*, 5562.
(60) Yang, H.; Lu, C.; Liu, Z.; Jin, H.; Che, Y.; Olmstead, M. M.; Balch, A. L. *J. Am. Chem. Soc.* **2008**, *130*, 17296.
(61) Lu, X.; Nakajima, K.; Iiduka, Y.; Nikawa, H.; Mizorogi, N.; Slanina, Z.; Tsuchiya, T.; Nagase, S.; Akasaka, T. *J. Am. Chem. Soc.* **2011**, *133*, 19553.
(62) Kurihara, H.; Lu, X.; Iiduka, Y.; Mizorogi, N.; Slanina, Z.; Tsuchiya, T.; Akasaka, T.; Nagase, S. *J. Am. Chem. Soc.* **2011**, *133*, 2382.
(63) Lu, X.; Nakajima, K.; Iiduka, Y.; Nikawa, H.; Tsuchiya, T.; Mizorogi, N.; Slanina, Z.; Nagase, S.; Akasaka, T. *Angew. Chem., Int. Ed.* **2012**, *51*, 5889.
(64) Popov, A. A.; Dunsch, L. *Chem.—Eur. J.* **2009**, *15*, 9707.
(65) Lu, J.; Zhang, X. W.; Zhao, X. G.; Nagase, S.; Kobayashi, K. *Chem. Phys. Lett.* **2000**, *332*, 219.
(66) Campanera, J. M.; Bo, C.; Olmstead, M. M.; Balch, A. L.; Poblet, J. M. *J. Phys. Chem. A* **2002**, *106*, 12356.
(67) Benson, D.; Li, Y.; Luo, W.; Ahuja, R.; Svensson, G.; Häussermann, U. *Inorg. Chem.* **2013**, *52*, 6402.
(68) Mayer, I. *Chem. Phys. Lett.* **1983**, *97*, 270.
(69) Mayer, I. *Int. J. Quantum Chem.* **1984**, *26*, 151.
(70) Bridgeman, A. J.; Cavigliasso, G.; Ireland, L. R.; Rothery, J. *J. Chem. Soc., Dalton Trans.* **2001**, 2095.
(71) Lu, T.; Chen, F. W. *J. Comput. Chem.* **2012**, *33*, 580.
(72) Popov, A. A. *J. Comput. Theor. Nanosci.* **2009**, *6*, 292.
(73) Tan, K.; Lu, X.; Wang, C. R. *J. Phys. Chem. B* **2006**, *110*, 11098.